Voltage Stability and Frequency Synchronization of Weak Power Distribution Networks with Inverter-Based Distributed Generators

Zhao Wang and Michael Lemmon [a],

[a] *Department of Electrical Engineering, University of Notre Dame, Notre Dame, IN 46556, USA*

Abstract

Inverter-based distributed generators (DGs), usually a part of microgrids, are incorporated to improve power quality and reliability when disruptions happen in main grid service. Due to multidirectional power flows caused by DGs, both voltage stability and frequency synchronization become significant issues when the network interconnections are *weak*. The weakness of a link usually means a significant resistive component in its impedance (*lossy*). In addition, a weak link has a large amount of power flowing through compared with the rated power level, so that the link is under stress. This paper derives sufficient conditions for voltage stability and frequency synchronization of a weak power distribution network coupled with inverter-based DGs. These conditions take the form of inequality constraints on network parameters, load levels and generation control commands. Simulation tests show that asymptotic voltage stability and frequency synchronization are ensured in a weak network, even after recovering from disturbances such as load changes and voltage impulses. Simulation also indicates that, strong network stability conditions, which consider no voltage control, do not apply to truly *weak* networks.

Key words: Weak networks, inverter-based distributed generator, voltage and frequency stability.

1 INTRODUCTION

Inverter-based distributed generation (DG) sources are usually a part of microgrids [13], together with other generation, storage and load units. These microgrids are installed to improve power quality and reliability, by supplying power locally during main grid contingency events. Power quality, in the form of voltage magnitude and network frequency, is the focus of power network operation. In addition to the lack of inertia of inverter-based DGs, connections of DGs introduce multidirectional power flows that cause power quality problems in weak networks. A *weak* network is typically defined in the sense of the ratio between resistance and reactance R/X, which is greater than one. Network weakness, however, also means a large power flow compared with the rated power level. From this perspective, a network weakness parameter called short-circuit ratio (SCR) is defined in [18], as the ratio between a bus' short-circuit power and its coupled generator's power rating. As a consequence of such weakness, dynamics of phase angles and voltages are coupled, which makes it difficult to simultaneously guarantee voltage stability and frequency synchronization.

Although a long-treated topic, existing stability analysis approaches are not sufficient to obtain both voltage control and frequency synchronization conditions in weak networks, especially with inverter-based DGs connected. Initial research efforts apply Lyapunov-based methods in [1] [5] [7] [26] to check transient frequency stability properties. These works focus on determining regions of stability in a network of rotating machine based generators. Although closed-form stability conditions are obtained, strong networks are assumed without voltage control dynamics, not proper for analyzing weak networks. To deal with weak networks, research works [12] [14] [24] checked small-signal stability through eigenvalue calculation of linearized network models. These efforts focus on computing eigenvalues for a large-scale system model, some taking advantage of sparse system matrices [24]. However, linearized analysis only applies to small neighborhoods of linearization points and are not in closed-form. Applying Lyapunov-based method to weak networks, a Hamiltonian structure-based method checks transient stability, where nonlinearity is maintained [20] [21]. Al-

⋆ Corresponding author Z. Wang. Tel. +01-574-631-3736.

Email address: zwang6, lemmon@nd.edu (Zhao Wang and Michael Lemmon).

though transient stability is naturally established with this passivity-based method, it is pointed out in [22] that not all nonlinear control systems can be transformed to a Hamiltonian control system, and the transformation is not trivial to find [21]. There have been no closed-form stability conditions for weak distribution networks coupled with DGs, with strong network assumptions relaxed. Even weak networks treated in these papers are merely *lossy*, where power flow stress is not considered. As an exception in [18], small-signal stability analysis shows that an increasing power flow stress leads to instability. A measure of network power flow stress (i.e. SCR) is used in this paper to treat truly *weak* networks.

The objective of this paper is to develop a comprehensive framework for assessing voltage stability and frequency synchronization of weak networks coupled with inverter-based DGs. Earlier work [8] has studied the stability of relatively strong networks with DGs, but, to our best knowledge, there has been little work examining both frequency synchronization and voltage control conditions for stressed weak networks. Some work [4] has attempted to address that issue by viewing the network as a set of coupled nonlinear oscillators, assuming voltages are kept within bounds. In their recent work [9], decoupled dynamics are incorporated and no voltage stability conditions are provided. Another recent paper [17] discusses frequency stability for an inverter-based microgrid. Stability is analyzed in a strong network with a large SCR (above 60). Building upon these prior works, this paper derives a set of inequality constraints whose satisfaction assures asymptotic voltage stability and frequency synchronization. Sufficient conditions are on network weakness, voltage control authority, and load levels. Stability analysis in this paper relaxes several key assumptions in the previous conference paper [25] and is further examined in a stressed weak network.

The remainder of this paper is organized as follows. Section 2 reviews the power system background and notational conventions used throughout this paper. Section 3 presents the weak network model, including voltage and frequency droop controllers. Section 4 presents the main results of this paper, i.e. sufficient conditions that ensure voltage stability and frequency synchronization. Section 5 demonstrates simulation results showing that satisfying stability conditions ensures asymptotic stability, while conditions derived for strong networks are not sufficient to stabilize weak networks. Section 6 provides concluding remarks and identifies future directions.

2 Background and Notations

This section reviews background knowledge, including power flow relationships and load models. Before the introduction, this paper makes two basic assumptions, i.e. three-phase balanced operation and per-unit normalization. Stability analyses in this paper build upon a balanced three-phase network model. In addition, per-unit (p.u.) normalization is applied to accommodate various nominal voltage levels within a network.

In a balanced three-phase network with n buses, impedance of a link between any bus i and bus j is $Z_{ij} = R_{ij} + jX_{ij}$. As defined in [2], when $Z_{ij} \neq 0$, there is $Y_{ij} = -1/Z_{ij}$; otherwise, there is $Y_{ij} = 0$. The diagonal element of Y is then $Y_{ii} = -\sum_{j=1, j\neq i}^{n} Y_{ij}$. This complex symmetric n-by-n admittance matrix $Y_{n\times n}$ is also expressed as $Y_{n\times n} = G_{n\times n} + jB_{n\times n}$, with conductance matrix $G_{n\times n}$ and susceptance matrix $B_{n\times n}$. For elements of the two symmetric real matrices $\{G_{ij}\}$ and $\{B_{ij}\}$, where $i, j \in \{1, 2, \ldots, n\}$: if $j = i$, then $G_{ii} > 0$ and $B_{ii} < 0$; if $j \neq i$, then there are $G_{ij} = G_{ji} \leq 0$ and $B_{ij} = B_{ji} \geq 0$.

Admittance matrix $Y_{n\times n}$ differs between weak and strong networks. Weak network has the ratio of $|R_{ij}/X_{ij}| \geq 1$ for the connection link between bus i and bus j, which is equivalent to $|G_{ij}/B_{ij}| \geq 1$. In contrast, strong networks are assumed to be with negligible G_{ij}, then there is a pure imaginary admittance matrix $Y_{n\times n} = jB_{n\times n}$, which simplifies the network model.

Besides a nontrivial real component G_{ij} in each admittance Y_{ij}, from the perspective of power flow stress, short-circuit ratio (SCR) is defined in [18] to characterize network weakness. SCR is the ratio between the short circuit power at a DG's point of common coupling and the DG's maximum apparent power. A network with an SCR smaller than 10 is considered to be *weak*, while one with SCR larger than 20 is termed as *strong*.

Power balance relationship is defined using $Y_{n\times n}$, depicting power exchanges between buses. Complex power vector S is defined as

$$S = P + jQ = VI^* = V(Y_{n\times n}V)^*, \tag{1}$$

in which P and Q are n-dimensional real and reactive power vectors; V and I are complex voltage and current vectors. Based on the power relation in equation (1), real power injection P_i and reactive power injection Q_i at bus i depend on states of neighboring buses, captured in the so called *power balance* relationships

$$P_i = \sum_{j=1}^{n} E_i E_j (G_{ij}\cos(\delta_i - \delta_j) + B_{ij}\sin(\delta_i - \delta_j)), \tag{2}$$

$$Q_i = \sum_{j=1}^{n} E_i E_j (G_{ij}\sin(\delta_i - \delta_j) - B_{ij}\cos(\delta_i - \delta_j)), \tag{3}$$

in which E_i is voltage magnitude and δ_i is phase angle at bus i. In weak networks, as shown in equations (2,3), the real and reactive power vectors are closely coupled through sinusoidal functions. In contrast, with

trivial $\{G_{ij}\}$ and phase shifts between buses, power balance relations in strong networks are simplified as $P_i = \sum_{j=1}^{n} E_i E_j B_{ij} \sin(\delta_i - \delta_j) \approx \sum_{j=1}^{n} E_i E_j B_{ij} (\delta_i - \delta_j)$ and $Q_i = -\sum_{j=1}^{n} E_i E_j B_{ij} \cos(\delta_i - \delta_j) \approx -\sum_{j=1}^{n} E_i E_j B_{ij}$.

Many research efforts take the simplified linear relations for simplicity. Nevertheless, DG-coupled distribution networks are weak, whose dynamics are coupled as in equations (2,3). This coupling nature in weak networks makes controlling DGs a challenging task, such as the "voltage rise problem" when DGs inject real power into a weak network.

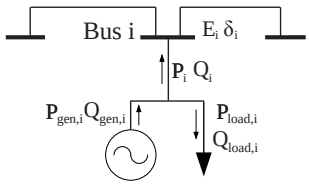

Fig. 1. Power Balance at Bus i

On any bus i, there is a controlled generator and a synthesized load, as shown in Figure 1. $P_{gen,i}$ and $Q_{gen,i}$ are the total powers generated at bus i. $P_{load,i}$ and $Q_{load,i}$ denote the real and reactive loads at bus i. Therefore the powers injected into bus i are

$$P_i = P_{gen,i} - P_{load,i}, \tag{4}$$
$$Q_i = Q_{gen,i} - Q_{load,i}. \tag{5}$$

Pure load bus i has $P_i + P_{load,i} = 0$ and $Q_i + Q_{load,i} = 0$.

A ZIP model is applied to approximate various types of loads [15] using a 2nd-order polynomial load model of voltage magnitudes $\{E_i\}$ in per units that combines constant impedance (Z), constant current (I) and constant power (P) components. Within expressions $P_{load,i} = E_i^2 P_{load,a,i} + E_i P_{load,b,i} + P_{load,c,i}$ and $Q_{load,i} = E_i^2 Q_{load,a,i} + E_i Q_{load,b,i} + Q_{load,c,i}$, $P_{load,a,i}$ and $Q_{load,a,i}$ are nominal constant impedance loads, e.g. incandescent light bulbs and resistance heaters; $P_{load,b,i}$ and $Q_{load,b,i}$ are nominal constant current loads, usually representing active motor controllers; $P_{load,c,i}$ and $Q_{load,c,i}$ are nominal constant power loads, generally a result of active power control.

3 System Model

This section obtains system models of DG-coupled weak networks. As the first step, conditions are derived to establish an isolated equilibrium point. Phase angle dynamic equations of a network are then constructed as nonlinear oscillators. With respect to the equilibrium point, voltage error dynamic equations are obtained. Definitions of frequency synchronization and voltage stability are then provided.

In this paper, inverter based controller designs are drawn from the CERTS (Consortium for Electric Reliability Technology Solutions) droop controller concepts [13], modified from conventional droop controllers. These controllers take advantage of differences between control commands and desired equilibrium points to balance power flows among multiple DGs. For m inverter-based DGs, the associated phase angle and voltage dynamic equations at the ith inverter-based DG are

$$\dot{\delta}_i = m_P(P_{ref,i} - P_{gen,i}) + \omega_0, \tag{6}$$
$$\dot{E}_i = K_Q(E_{ref,i} - E_i) - m_Q Q_{gen,i}, \tag{7}$$

for all $i \in \{1, 2, \ldots, m\}$, where m_P is the droop slope of P-f droop controller; ω_0 is the nominal angular frequency; K_Q is the voltage control gain of Q-E droop controller; m_Q is the droop slope of Q-E droop controller. In equations, $P_{ref,i}$ and $E_{ref,i}$ denote the commanded real power and voltage levels of the controller. The complete system model is obtained in equations (2-7).

To define equilibrium points of the complete system model in equations (2-7), a change of variable is necessary to remove one surplus degree of freedom (DOF) in phase angles $\{\delta_i\}$. In a network with m DG-coupled buses, phase angles of the first $(m-1)$ buses refer to a common bus, i.e. the mth bus. Define phase angle difference $\theta_i = \delta_i - \delta_m$ for all $i \in \{1, 2, \ldots, m-1\}$ and $\theta_m = 0$. The equilibrium is expressed as $(P_{equ}, Q_{equ}, \theta_{equ}, E_{equ}, \omega_{equ})$, which is a zero point of the dynamic equations. Corresponding to a total number of $2m$ unknown states $(E_{equ}, \theta_{equ}, \omega_{equ})$, there are $2m$ equations $f(t) = [f_1; f_2; f_3]^T = 0$, where f_1, f_2, and f_3 are as follows

$$f_{1,i} = K_Q(E_{ref,i} - E_{equ,i}) - m_Q(Q_{equ,i} + Q_{load,i}), \quad i \in \{1, \ldots, m\} \tag{8}$$
$$f_{2,i} = m_P[(P_{ref,i} - P_{equ,i} - P_{load,i}) - (P_{ref,m} - P_{equ,m} - P_{load,m})], \quad i \in \{1, \ldots, m-1\} \tag{9}$$
$$f_3 = \omega_0 - \omega_{equ} + m_P(P_{ref,m} - P_{equ,m} - P_{load,m}). \tag{10}$$

Asymptotic stability can be discussed with respect to $(P_{equ}, Q_{equ}, \theta_{equ}, E_{equ}, \omega_{equ})$, as long as it is isolated. The following lemma establishes the existence of an isolated equilibrium point through Jacobian matrix of equations (8-10).

Lemma 1 *For any given real power $\{P_{ref,i}\}$ and voltage $\{E_{ref,i}\}$ commands, if Jacobian matrices $\frac{\partial f_1}{\partial E_{equ}}$, $\frac{\partial f_2}{\partial \theta_{equ}}$, as well as matrices $(I - (\frac{\partial f_1}{\partial E_{equ}})^{-1} \frac{\partial f_1}{\partial \theta_{equ}} (\frac{\partial f_2}{\partial \theta_{equ}})^{-1} \frac{\partial f_2}{\partial E_{equ}})$ and $(I - (\frac{\partial f_2}{\partial \theta_{equ}})^{-1} \frac{\partial f_2}{\partial E_{equ}} (\frac{\partial f_1}{\partial E_{equ}})^{-1} \frac{\partial f_1}{\partial \theta_{equ}})$ are full rank, then there is an isolated equilibrium point $(P_{equ}, Q_{equ}, \theta_{equ}, E_{equ}, \omega_{equ})$ for the complete system model in equations (2,3,8-10).*

Proof 1 *Jacobian of the nonlinear function* $f(t) = [f_1; f_2; f_3]^T$ *in equations (8-10) is as follows:*

$$J = \left(\begin{array}{c|cc} \frac{\partial f_1}{\partial E_{equ}} & \frac{\partial f_1}{\partial \theta_{equ}} & 0 \\ \hline \frac{\partial f_2}{\partial E_{equ}} & \frac{\partial f_2}{\partial \theta_{equ}} & 0 \\ \frac{\partial f_3}{\partial E_{equ}} & \frac{\partial f_3}{\partial \theta_{equ}} & -1 \end{array}\right),$$

whose determinant is $det(\frac{\partial f_1}{\partial E_{equ}})\ det(\frac{\partial f_2}{\partial \theta_{equ}})\ det(I - (\frac{\partial f_2}{\partial \theta_{equ}})^{-1}\frac{\partial f_2}{\partial E_{equ}}(\frac{\partial f_1}{\partial E_{equ}})^{-1}\frac{\partial f_1}{\partial \theta_{equ}})$ *or equivalently* $det(\frac{\partial f_2}{\partial \theta_{equ}})\ det(\frac{\partial f_1}{\partial E_{equ}})\ det(I - (\frac{\partial f_1}{\partial E_{equ}})^{-1}\frac{\partial f_1}{\partial \theta_{equ}}(\frac{\partial f_2}{\partial \theta_{equ}})^{-1}\frac{\partial f_2}{\partial E_{equ}})$. *The Jacobian maintains its rank, iff matrix* $\frac{\partial f_1}{\partial E_{equ}}$, $\frac{\partial f_2}{\partial \theta_{equ}}$, *as well as matrices* $(I - (\frac{\partial f_1}{\partial E_{equ}})^{-1}\frac{\partial f_1}{\partial \theta_{equ}}(\frac{\partial f_2}{\partial \theta_{equ}})^{-1}\frac{\partial f_2}{\partial E_{equ}})$ *and* $(I - (\frac{\partial f_2}{\partial \theta_{equ}})^{-1}\frac{\partial f_2}{\partial E_{equ}}(\frac{\partial f_1}{\partial E_{equ}})^{-1}\frac{\partial f_1}{\partial \theta_{equ}})$ *are full rank. Based on implicit function theorem in [6], within a small neighborhood where the Jacobian is full rank, there is an isolated equilibrium* $(P_{equ}, Q_{equ}, \theta_{equ}, E_{equ}, \omega_{equ})$.

An equilibrium point $(P_{equ}, Q_{equ}, \theta_{equ}, E_{equ}, \omega_{equ})$ is achieved through commands $\{P_{ref,i}\}$ and $\{E_{ref,i}\}$, designated to droop controllers. This equilibrium point is usually determined as a solution to some optimal power flow (OPF) problems. Based on equations (8-10), voltage and real power reference commands are then determined as

$$E_{ref,i} = E_{equ,i} + \frac{m_Q}{K_Q}(Q_{equ,i} + Q_{load,i}(E_{equ})), \quad (11)$$

$$P_{ref,i} = P_{equ,i} + P_{load,i}(E_{equ}) + \frac{1}{m_P}(\omega_{equ} - \omega_0), \quad (12)$$

for all $i \in \{1, 2, \ldots, m\}$. The following assumption is about the existence of an isolated equilibrium point:

Assumption 1 *Each* $(P_{equ}, Q_{equ}, \theta_{equ}, E_{equ}, \omega_{equ})$, *as a solution to some OPF problem, is assumed to satisfy the conditions in Lemma 1, so that it is an isolated equilibrium point in a small neighborhood.*

To derive a more general model for frequency synchronization analysis, phase angle dynamics in equation (6) are formulated as nonlinear oscillators. By inserting equations (2,4) into equation (6), there is

$$\begin{aligned}\dot{\delta}_i &= m_P(P_{ref,i} - P_i - P_{load,i}) + \omega_0,\\ &= \omega_0 + m_P(P_{ref,i} - E_i^2 G_{ii} - P_{load,i}(E_i))\\ &\quad - m_P \sum_{j=1, j\neq i}^{n} E_i E_j (G_{ij}\cos(\delta_i - \delta_j) + B_{ij}\sin(\delta_i - \delta_j)),\\ &= \omega_i - m_P \sum_{j=1, j\neq i}^{n} E_i E_j |Y_{ij}| \sin(\delta_i - \delta_j + \phi_{ij}), \end{aligned} \quad (13)$$

for all $i \in \{1, 2, \ldots, m\}$, where the natural frequency is $\omega_i = \omega_0 + m_P(P_{ref,i} - E_i^2 G_{ii} - P_{load,i}(E_i))$; phase shift between bus i and j, $\phi_{ij} = \phi_{ji} = \tan^{-1}(G_{ij}/B_{ij}) \in [-\frac{\pi}{2}, 0]$; the diagonal terms are $|Y_{ii}| = 0$ and $\phi_{ii} = 0$.

A typical n-bus distribution network includes m DG-coupled buses and l pure load buses, which is modeled as a hybrid network as follows

$$\begin{aligned}\dot{\delta}_i &= \omega_i - m_P \sum_{j=1, j\neq i}^{n} E_i E_j |Y_{ij}| \sin(\delta_i - \delta_j + \phi_{ij}),\\ &\quad i \in \{1, \ldots, m\}\\ \dot{\delta}_i &= \frac{\sum_{j=1, j\neq i}^{n} E_i E_j |Y_{ij}| \cos(\delta_i - \delta_j + \phi_{ij})\dot{\delta}_j}{\sum_{j=1, j\neq i}^{n} E_i E_j |Y_{ij}| \cos(\delta_i - \delta_j + \phi_{ij})},\\ &\quad i \in \{m+1, \ldots, m+l\}\end{aligned}$$

where $\omega_i = \omega_0 + m_P(P_{ref,i} - E_i^2 G_{ii} - P_{load,i}(E))$ is the natural frequency at bus i. Based on the hybrid network of nonlinear oscillators above, frequency synchronization is defined as asymptotic convergence of network frequency, as follows

Definition 2 *The power distribution network has frequency synchronization if there are two open subsets of* $\Omega_{E,1}, \Omega_{\theta,1} \subset \mathbb{R}^n$ *containing the origin such that if any* $\tilde{E}_i(0) \in \Omega_{E,1}$ *and any* $\theta_i(0) = (\delta_i(0) - \delta_n(0)) \in \Omega_{\theta,1}$ *then* $\lim_{t\to\infty} \dot{\delta}_1(t) = \ldots = \lim_{t\to\infty} \dot{\delta}_n(t) = \omega_{equ}$, *when the inputs* P_{ref}, $P_{load,a}$, $P_{load,b}$, $P_{load,c}$, E_{ref}, $Q_{load,a}$, $Q_{load,b}$, $Q_{load,c}$ *are constant.*

Voltage control dynamic model is based on the isolated equilibrium point that satisfies conditions in *Lemma* 1. Given an isolated equilibrium point, error states are defined for phase angle, voltage magnitude and reactive power error vectors as $\tilde{\theta} = \theta - \theta_{equ}$, $\tilde{E} = E - E_{equ}$, and $\tilde{Q} = Q_{equ} - Q$. Voltage error dynamics model is:

$$\begin{aligned}\dot{\tilde{E}}_i &= \dot{E}_i - \dot{E}_{equ,i},\\ &= -K_Q\tilde{E}_i + m_Q\tilde{Q}_i) + m_Q(Q_{load,i}(E_{equ,i}) - Q_{load,i}(E_i)),\\ &= m_Q\tilde{Q}_i - \{K_Q + m_Q[Q_{load,b,i} + (E_{equ,i} + E_i)Q_{load,a,i}]\}\tilde{E}_i,\\ &= m_Q\tilde{Q}_i - m_Q Q_{load,a,i}\tilde{E}_i{}^2\\ &\quad - m_Q[\frac{K_Q}{m_Q} + (Q_{load,b,i} + 2Q_{load,a,i}E_{equ,i})]\tilde{E}_i, \quad (14)\\ &\quad i \in \{1, 2, \ldots, m\}\\ \tilde{Q}_i &= Q_{load,a,i}\tilde{E}_i^2 + (2Q_{load,a,i}E_{equ,i} + Q_{load,b,i})\tilde{E}_i. \quad (15)\\ &\quad i \in \{m+1, \ldots, m+l\}\end{aligned}$$

Equation (15) shows an algebraic relation between voltage magnitude and reactive power error vectors for pure load buses. With respect to the voltage error dynamics model above, it is possible to define voltage stability of the power distribution network, as follows

Definition 3 *The power distribution network has voltage stability if there are two open subsets of* $\Omega_{E,2}, \Omega_{\theta,2} \subset \mathbb{R}^n$ *containing the origin such that if any* $\tilde{E}_i(0) \in \Omega_{E,2}$ *and any* $\theta_i(0) = (\delta_i(0) - \delta_n(0)) \in \Omega_{\theta,2}$ *then* $\lim_{t\to\infty} \tilde{E}_1(t) = \ldots = \lim_{t\to\infty} \tilde{E}_n(t) = 0$*, when the inputs* P_{ref}*,* $P_{load,a}$*,* $P_{load,b}$*,* $P_{load,c}$*,* Q_{ref}*,* $Q_{load,a}$*,* $Q_{load,b}$*,* $Q_{load,c}$ *are constant.*

In conclusion, the stability analysis problem treated in this paper considers both asymptotic frequency synchronization to ω_{equ} and voltage control to E_{equ}. In section 4, sufficient conditions are derived for stability in *Definition* 2 and 3.

4 Main Result

This section derives sufficient conditions for voltage stability and frequency synchronization in DG-coupled distribution networks. As long as these conditions are satisfied, the network asymptotically converges to the designated equilibrium point, within regulatory limits. Stability analysis is then discussed in a grid-connected network scenario, addressing concerns of how to manage DGs.

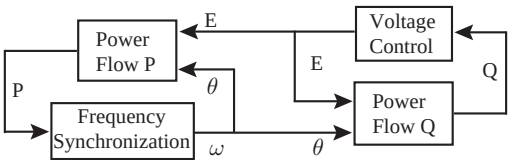

Fig. 2. Complete Model of the Network

The coupling nature of voltage control and frequency synchronization is solved by segmenting the entire system model into four interconnected blocks, as shown in Figure 2, including a voltage control block, a frequency synchronization block, and two power balance blocks. Stability analysis then decouples by first identifying the existence of voltage magnitude and phase angle invariant sets; then proving asymptotic stability of both phase angle differences and voltages; finally establishing frequency synchronization. Stability analysis in this paper does not require a DG connected to each bus, as required in [25].

4.1 Invariant Sets

With no assumption on phase angles' differences θ, a positive invariant set of voltage magnitudes $\mathcal{I}_E$ is identified. Only two subsystems, i.e. the "Power Flow Q" block and the "Voltage Control" block, are involved to prove bounded voltage magnitudes. Since relationships are purely algebraic between voltage and reactive power errors on pure load buses as shown in equation (15), only dynamics on DG-connected buses are considered. The following lemma characterizes a positive invariant set of voltage magnitudes $\mathcal{I}_E$.

Lemma 2 *Consider the system model in equations (2,3,13-15), with* $|\tilde{\theta}_i| \leq 2\pi$ *for any* $i \in \{1, 2, \ldots, m\}$*. Given*

$$|Q_{load,a,i}| < a, \tag{16}$$

$$K_Q/m_Q > \max(b_1 - Q_{load,b,i} + 2\sqrt{(a - Q_{load,a,i})c}, -b_2 - Q_{load,b,i} + 2\sqrt{(Q_{load,a,i} + a)c}), \tag{17}$$

where

$$a = (2 + 4\pi)|G_{ii}|_{max} + (4 + 4\pi)|B_{ii}|_{max}, \tag{18}$$

$$b_1 = ((2 + 8\pi)|G_{ii}|_{max} + (4 + 8\pi)|B_{ii}|_{max} - 2Q_{load,a,i}) \max_i(E_{equ,i}), \tag{19}$$

$$b_2 = ((2 + 8\pi)|G_{ii}|_{max} + (4 + 8\pi)|B_{ii}|_{max} + 2Q_{load,a,i}) \max_i(E_{equ,i}), \tag{20}$$

$$c = 4\pi(|G_{ii}|_{max} + |B_{ii}|_{max})(\max_i(E_{equ,i}))^2. \tag{21}$$

If for each voltage magnitude E_i*,*

$$\tilde{E}_{-,l} \leq E_i(0) - E_{equ,i} \leq \tilde{E}_{+,u}, \tag{22}$$

then there exists a non-empty set

$$\mathcal{I}_E = \{E \in \mathbb{R}^m : E_{min} \leq E_i \leq E_{max}, 0 < E_{min} < E_{max}\},$$

where there are

$$E_{min} = \min_i(E_{equ,i}) + \min(0, \tilde{E}_{-,u}),$$

$$E_{max} = \max_i(E_{equ,i}) + \max(0, \tilde{E}_{+,l}),$$

and

$$\tilde{E}_{+,u} = \frac{K_Q/m_Q + Q_{load,b,i} - b_1}{2(a - Q_{load,a,i})} + \frac{\sqrt{(b_1 - K_Q/m_Q - Q_{load,b,i})^2 - 4(a - Q_{load,a,i})c}}{2(a - Q_{load,a,i})},$$

$$\tilde{E}_{+,l} = \frac{K_Q/m_Q + Q_{load,b,i} - b_1}{2(a - Q_{load,a,i})} - \frac{\sqrt{(b_1 - K_Q/m_Q - Q_{load,b,i})^2 - 4(a - Q_{load,a,i})c}}{2(a - Q_{load,a,i})},$$

$$\tilde{E}_{-,u} = -\frac{K_Q/m_Q + Q_{load,b,i} + b_2}{2(Q_{load,a,i} + a)} + \frac{\sqrt{(b_2 + K_Q/m_Q + Q_{load,b,i})^2 - 4(Q_{load,a,i} + a)c}}{2(Q_{load,a,i} + a)},$$

$$\tilde{E}_{-,l} = -\frac{K_Q/m_Q + Q_{load,b,i} + b_2}{2(Q_{load,a,i} + a)} - \frac{\sqrt{(b_2 + K_Q/m_Q + Q_{load,b,i})^2 - 4(Q_{load,a,i} + a)c}}{2(Q_{load,a,i} + a)}.$$

The nonempty set $\mathcal{I}_E$ is positively invariant with respect to equations (2,3,13-15).

Proof 4 *$\mathcal{I}_E$ will be an invariant set, if for arbitrary $i \in \{1, 2, \dots m\}$, $|\tilde{E}_i|$ is non-increasing on the border of $\mathcal{I}_E$, with two cases to be considered. When there is $\tilde{E}_i = E_i - E_{equ,i} > 0$. Inserting equation (A.1) into equation (14) yields*

$$\begin{aligned}\dot{\tilde{E}}_i \leq & -[K_Q + m_Q(2E_{equ,i} + \tilde{E}_i)Q_{load,a,i} + Q_{load,b,i}]\tilde{E}_i \\ & + m_Q(l_E\tilde{E}_i + l_\delta 2\pi), \\ = & \, m_Q c + m_Q(-K_Q/m_Q - Q_{load,b,i} + b_1)\tilde{E}_i \\ & + m_Q(-Q_{load,a,i} + a)\tilde{E}_i^2.\end{aligned}$$

$\dot{\tilde{E}}_i$ should be non-positive to make $\tilde{E}_i$ non-increasing. Given the lemma's hypothesis (16,17), the equation $(-Q_{load,a,i}+a)x^2+(-K_Q/m_Q-Q_{load,b,i}+b_1)x+c=0$ has two real solutions, at least one of them being positive. If $\tilde{E}_{+,l} \leq \tilde{E}_i \leq \tilde{E}_{+,u}$ is satisfied, then $\tilde{E}_i$ is not increasing when $\tilde{E}_i > 0$.

The other case is $\tilde{E}_i < 0$. Similarly,

$$\begin{aligned}\dot{\tilde{E}}_i \geq & -[K_Q + m_Q(2E_{equ,i} + \tilde{E}_i)Q_{load,a,i} + Q_{load,b,i}]\tilde{E}_i \\ & - m_Q(l_E\tilde{E}_i + l_\delta 2\pi), \\ = & -m_Q c - m_Q(K_Q/m_Q + Q_{load,b,i} + b_2)\tilde{E}_i \\ & - m_Q(Q_{load,a,i} + a)\tilde{E}_i^2.\end{aligned}$$

$\dot{\tilde{E}}_i$ should be non-negative to make $\tilde{E}_i$ non-decreasing. Given the lemma's hypothesis (16,17), the equation $(Q_{load,a,i}+a)x^2+(K_Q/m_Q+Q_{load,b,i}+b_2)x+c=0$ has two real solutions, at least one of them being negative. If $\tilde{E}_{-,l} \leq \tilde{E}_i \leq \tilde{E}_{-,u}$ is satisfied, then $\tilde{E}_i$ is non-decreasing when $\tilde{E}_i < 0$.

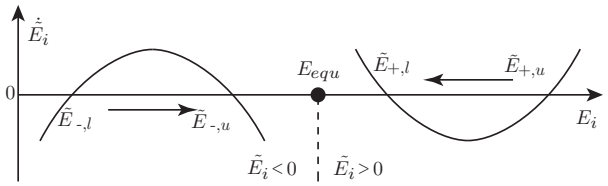

Fig. 3. Illustration of Voltage Invariant Set

Existence of an invariant set of voltage is demonstrated in Figure 3. The x-axis in the figure is the voltage magnitude E_i at bus i, and the y-axis is the derivative of voltage error $\dot{\tilde{E}}_i$. Separated by $E_{equ,i}$, voltage error dynamics are discussed with both $\tilde{E}_i < 0$ and $\tilde{E}_i > 0$. If conditions in equations (16,17) are satisfied, two quadratic curves cross the x-axis where $\dot{\tilde{E}}_i = 0$. When $\tilde{E}_i > 0$, there is a convex quadratic curve, with cross points $\{\tilde{E}_{+,l}, \tilde{E}_{+,u}\}$. When $\tilde{E}_i < 0$, there is a concave quadratic curve, with cross points $\{\tilde{E}_{-,l}, \tilde{E}_{-,u}\}$. If an initial voltage error $\tilde{E}_i(0)$ lies between either $\{\tilde{E}_{+,l}, \tilde{E}_{+,u}\}$ or $\{\tilde{E}_{-,l}, \tilde{E}_{-,u}\}$, $E_i(t)$ approaches to cross points that are closer to E_{equ}, i.e. with $\tilde{E}_{+,l}$ and $\tilde{E}_{-,u}$ respectively. For any $i \in \{1, 2, \dots, m\}$, $\tilde{E}_i$ stays in $\mathcal{I}_E$ once it starts between $\tilde{E}_{-,l}$ and $\tilde{E}_{+,u}$. Therefore, the two conditions in equations (22) imply that $\mathcal{I}_E$ is positively invariant.

Remark 1 *Equation (16) bounds constant impedance reactive load $Q_{load,a,i}$ by the coupling strength of the network through $|G_{ii}|_{max}$ and $|B_{ii}|_{max}$.*

Remark 2 *Equation (17) bounds worst-case voltage control authority K_Q/m_Q in the form of functions of reactive loads $Q_{load,i}$, voltage states $E_{equ,i}$, and network coupling (in G_{ii} and B_{ii}). It means that voltage control authority of DGs must compensate for local reactive loads and coupling from neighboring buses.*

As voltages are bounded within $\mathcal{I}_E$, a condition is determined for a positive invariant set of phase angles. The "Power Flow P" block and the "Frequency Synchronization" block, in Figure 2, are involved to prove bounded phase angle differences. The following lemma characterizes a positive invariant set of phase angle differences $\{\theta_i\}$, drawing upon techniques used in [4][3], based on consensus of nonlinear oscillators.

Lemma 3 *Assume the conditions in* Lemma *2 are satisfied.*

$$\begin{aligned}&\textit{Define } A_1 = nE_{\min}^2 \min_{i\neq j}(|B_{ij}|), \\ &\quad \textit{and } A_2 = \max_{i\neq j}(|\omega_i - \omega_j|) - 2E_{min}^2|G_{ii}|_{min}, \\ &\textit{in which } \omega_i = \omega_0 + m_P(P_{ref,i} - E_i^2 G_{ii} - P_{load,i}(E_i)),\end{aligned}$$

where $E_{\min}$ and $E_{\max}$ are from the set $\mathcal{I}_E$ in Lemma *2. If*

$$A_1 \sin(\theta) \geq A_2, \tag{23}$$

then there exists a non-empty set

$$\mathcal{I}_\theta = \{\theta \in \mathbb{R}^m : \max_{i,j}(|\theta_i - \theta_j|) \leq \theta, \theta \in [0, \pi]\},$$

which is positively invariant with respect to equations (2,3,13-15).

Proof 5 *Define a positive function $V_\theta(\theta) : \mathbb{R}^m \to [0, \pi]$ for the network with m buses as*

$$V_\theta(\theta) = \frac{1}{m_P}\max_{i\neq j}(|\theta_i - \theta_j|) = \frac{1}{m_P}(\theta_k - \theta_l),$$

where the kth bus achieves clockwise maximum θ_k and the lth bus achieves the counterclockwise minimum θ_l, with $k, l \in \{1, 2, \dots, m\}$. Assume that $|\theta_i(0) - \theta_j(0)| \leq \theta$

for any $i, j \in \{1, 2, \ldots, m\}$, where θ is arbitrary and $\theta \in [0, \pi]$, such that all angles are contained in an arc of length θ. The positive function V_θ only takes into account buses with inverter-based DGs, because pure load buses have their phase angle dynamics determined by neighboring buses. Once states on DG-coupled buses are obtained, states on pure load buses are derived through algebraic relationships.

Taking the upper Dini derivative of V_θ to deal with discontinuity, there is

$$\begin{aligned}
&D^+V_\theta \\
&= (\omega_k - \omega_l) \\
&- [\sum_{\substack{j=1 \\ j\neq k}}^{n} E_k E_j B_{kj} \sin(\theta_k - \theta_j) - \sum_{\substack{j=1 \\ j\neq l}}^{n} E_l E_j B_{lj} \sin(\theta_l - \theta_j)] \\
&- [\sum_{\substack{j=1 \\ j\neq k}}^{n} E_k E_j G_{kj} \cos(\theta_k - \theta_j) - \sum_{\substack{j=1 \\ j\neq l}}^{n} E_l E_j G_{lj} \cos(\theta_l - \theta_j)], \\
&\leq \max_{i\neq j}(|\omega_i - \omega_j|) - E_{\min}^2 n \min_{i\neq j}(|B_{ij}|) \sin\theta - 2E_{\min}^2 |G_{ii}|_{min}.
\end{aligned}$$

Under the lemma's assumption in equation (23), it is clear that $D^+V_\theta \leq 0$ and therefore V_θ is non-increasing. As a result, $\mathcal{I}_\theta$ is a positively invariant set.

Remark 3 *Equation (23) bounds network weakness in the form of B_{ij} and G_{ii}, while the size of phase angle invariant set is larger for strong networks than weak ones. Smaller natural frequency differences lead to easier convergence of phase angle differences.*

Existences of these two positive invariant sets $\mathcal{I}_E$ and $\mathcal{I}_\theta$ provide bounded voltage magnitudes and phase angle differences. Asymptotic convergence of phase angle differences and voltages are then proved, followed by frequency synchronization.

4.2 Asymptotic Stability

Before proving asymptotic stability, the following lemma is established to show that a reduced-ordered Metzler matrix [23] with zero row sums still has the same property. It is used when pure load buses are considered in frequency synchronization analysis.

Lemma 4 *Assume that F is a Metzler matrix with zero row sums, if matrix F is written as a block matrix as $[F_1 \quad F_2; F_3 \quad F_4]$, in which F_2 and F_3 have non-zero elements on each row, then the matrix $(F_1 - F_2F_4^{-1}F_3)$ is also a Metzler matrix with zero row sums.*

Proof 6 *Since the matrix F is a Metzler matrix with zero row sums, then there is*

$$F_{ii} + \sum_{j=1, j\neq i}^{n} F_{ij} = 0, \quad |F_{ii}| = \sum_{j=1, j\neq i}^{n} F_{ij} = 0.$$

Based on Gershgorin theorem, matrix F has all its eigenvalue disks centered at diagonal component values stay complete in the left-hand-side of the imaginary axis.

Because matrix F_2 has non-zero elements on each row, diagonal block matrices F_1 have its row sums as follows

$$\begin{aligned}
F_{1,ii} + \sum_{j=1, j\neq i}^{m} F_{1,ij} &= -\sum_{j=1, j\neq i}^{l} F_{2,ij} < 0, \\
|F_{1,ii}| &> \sum_{j=1, j\neq i}^{n} F_{1,ij} > 0.
\end{aligned}$$

Also based on Gershgorin theorem, matrix F_1 has all its eigenvalues with negative real parts. Similarly, matrix F_4 also has all its eigenvalues with negative real parts. Diagonal block matrices F_1 and F_4 are both invertible.

Since matrix $(-F_4)$ is a nonsingular matrix with negative off-diagonal entries, whose eigenvalues all have positive real parts, then $(-F_4)$ is an M-matrix [16]. Based on characteristics of M-matrices, its inverse $(-F_4)^{-1}$ is nonnegative with all its elements nonnegative. Therefore, matrix F_4 is invertible, and all elements of the inverse matrix F_4^{-1} are negative.

Expressing F_4 and F_4^{-1} in row vectors $\{b_i\}$ and column vectors $\{a_i\}$, respectively, where $i \in \{1, \ldots, l\}$. Equation $F_4F_4^{-1} = F_4^{-1}F_4 = I$ is rewritten as

$$F_4^{-1}F_4 = \begin{pmatrix} b_1 \\ b_2 \\ \vdots \\ b_l \end{pmatrix} \begin{pmatrix} a_1 & a_2 & \ldots & a_l \end{pmatrix} = \begin{pmatrix} 1 & 0 & \ldots & 0 \\ 0 & 1 & \ldots & 0 \\ \vdots & \vdots & \ddots & \vdots \\ 0 & 0 & \ldots & 1 \end{pmatrix},$$

then $b_i \sum_{i=1}^{l} a_i = 1$ for each $i \in \{1, 2, \ldots, l\}$. Expressing F_3 in column vectors $\{c_j\}$, where $j \in \{1, \ldots, m\}$, then there is

$$F_4^{-1}F_3 = \begin{pmatrix} b_1 \\ b_2 \\ \vdots \\ b_l \end{pmatrix} \begin{pmatrix} c_1 & c_2 & \ldots & c_m \end{pmatrix} = \begin{pmatrix} d_1 & d_2 & \ldots & d_m \end{pmatrix},$$

whose row sums are $b_i \sum_{i=1}^{m} c_i$ for all $i \in \{1, 2, \ldots, l\}$. Since each column vector c_i are positive, b_ic_j is negative

for any i and j. Since F is a Metzler matrix with zero row sums, there is $\sum_{j=1}^{m} c_j + \sum_{j=1}^{l} a_j = 0$ for each $i \in \{1, 2, \ldots, l\}$, then each row sum has $b_i \sum_{j=1}^{m} c_j = -b_i \sum_{j=1}^{l} a_j = -1$. Since $b_i \sum_{j=1}^{m} c_j = -1$ and each $b_i c_j$ is negative, then there is $-1 \leq b_i c_j \leq 0$ and matrix $F_4^{-1} F_3$ has all its components negative. With matrix F_2 expressed as row vectors $\{e_j\}$, where $j \in \{1, \ldots, m\}$, then there is a square matrix

$$F_2 F_4^{-1} F_3 = \begin{pmatrix} e_1 d_1 & e_1 d_2 & \ldots & e_1 d_m \\ e_2 d_1 & e_2 d_2 & \ldots & e_2 d_m \\ \vdots & \vdots & \ddots & \vdots \\ e_m d_1 & e_m d_2 & \ldots & e_m d_m \end{pmatrix}.$$

Since each element of vector d_j is between -1 and 0, then there is $0 \leq -e_i d_i \leq \sum_{j=1}^{m} e_j$. Expressing matrix F_1 as row vectors $\{f_j\}$, then there is

$$F_1 - F_2 F_4^{-1} F_3 = \begin{pmatrix} f_1 \\ f_2 \\ \vdots \\ f_m \end{pmatrix} - \begin{pmatrix} e_1 d_1 & e_1 d_2 & \ldots & e_1 d_m \\ e_2 d_1 & e_2 d_2 & \ldots & e_2 d_m \\ \vdots & \vdots & \ddots & \vdots \\ e_m d_1 & e_m d_2 & \ldots & e_m d_m \end{pmatrix},$$

in which each row is $f_i 1_m - e_i \sum_{i=1}^{m} d_i = 0$. Since there is $f_{ii} - e_i d_i \leq f_{ii} + \sum_{j=1}^{m} e_j \leq 0$, then each diagonal element $(f_{ii} - e_i d_i)$ is non-positive and all non-diagonal elements $f_{ij} - e_i d_j$ are positive. As a result, the matrix $F_1 - F_2 F_4^{-1} F_3$ is still a Metzler matrix with zero row sums.

Building upon the two invariant sets $\mathcal{I}_E$ and $\mathcal{I}_\theta$, asymptotic convergence of phase angle differences θ requires a stricter condition than the one in *Lemma* 3. The following theorem establishes sufficient conditions for phase angle differences convergence.

Theorem 7 *Under conditions in* Lemma *2 and 3, if*

$$A_1 \sin(\pi/2 - \alpha_{\max}) \geq A_2, \quad (24)$$
$$\text{in which } A_1 = n E_{\min}^2 \min_{i \neq j}(|B_{ij}|),$$
$$\text{and } A_2 = \max_{i \neq j}(|\omega_i - \omega_j|) - 2E_{min}^2 |G_{ii}|_{min},$$

where $\alpha_{\max} = \max_{i \neq j}(\tan^{-1}(-G_{ij}/B_{ij}))$, then each phase angle $\lim_{t \to \infty} \theta_i(t) = \theta_{equ,i}$, for all $i \in \{1, 2, \ldots, m\}$.

Proof 8 *It is assumed that voltage magnitudes are constants and phase angles are states changing with time. Define $\alpha_{ij} = -\phi_{ij} = \tan^{-1}(-\frac{G_{ij}}{B_{ij}}) \in [0, \frac{\pi}{2}]$. Because natural frequency $\omega_i = \omega_0 + m_P(P_{ref,i} - E_i^2 G_{ii} - P_{load,i}(E_i))$ for bus i, it is not a function of phase angles δ_i. Taking voltages as inputs, derivatives of equation (13) are*

$$\begin{aligned} \frac{d\dot{\delta}_i}{dt} &= -m_P \sum_{\substack{j=1 \\ j \neq i}}^{n} E_i E_j |Y_{ij}| \cos(\delta_i - \delta_j - \alpha_{ij})(\dot{\delta}_i - \dot{\delta}_j) \\ &= m_P F_i(t) \dot{\delta}, \end{aligned}$$

for $i \in \{1, 2, \ldots, m\}$, where F is a matrix whose components are

$$\begin{aligned} F_{ii}(t) &= -\sum_{\substack{j=1 \\ j \neq i}}^{n} E_i E_j |Y_{ij}| \cos(\delta_i - \delta_j - \alpha_{ij}), \\ F_{ij}(t) &= E_i E_j |Y_{ij}| \cos(\delta_i - \delta_j - \alpha_{ij}). \end{aligned}$$

Similarly for pure load buses, since $P_i + P_{load,i} = 0$ and $P_{load,i}$ is independent of frequency, then there is

$$0 = -\sum_{\substack{j=1 \\ j \neq i}}^{n} E_i E_j |Y_{ij}| \cos(\delta_i - \delta_j - \alpha_{ij})(\dot{\delta}_i - \dot{\delta}_j) = F_i(t) \dot{\delta},$$

for $i \in \{m+1, m+2, \ldots, m+l\}$, where $F(t)$ has the same form as the fast inverters.

By Lemma *3 and setting $\theta = \frac{\pi}{2} - \alpha_{max}$, for all $\theta_i, \theta_j \in \mathcal{I}_\theta$ where $i, j \in \{1, 2, \ldots, n\}$, there is $|\theta_i - \theta_j| = |\delta_i - \delta_j| < \frac{\pi}{2} - \alpha_{\max}$. This inequality simply means that $\cos(\delta_i - \delta_j - \alpha_{ij}) > 0$, then matrix $F(t)$ satisfies: (a) its off-diagonal elements are nonnegative and (b) its row sums are zero. As a result, $F(t)$ is a Metzler matrix with zero row sums for every time instant t.*

With both dynamics of inverter-based DGs and pure load buses, the complete system model is as follows, .

$$\begin{aligned} \frac{d}{dt} \begin{pmatrix} \dot{\delta}_{m \times 1} \\ \dot{\delta}_{l \times 1} \end{pmatrix} &= \begin{pmatrix} \frac{d}{dt} \dot{\delta}_{m \times 1} \\ 0_{l \times 1} \end{pmatrix} \\ &= \begin{pmatrix} m_P F_1 & m_P F_2 \\ F_3 & F_4 \end{pmatrix} \begin{pmatrix} \dot{\delta}_{m \times 1} \\ \dot{\delta}_{l \times 1} \end{pmatrix}. \end{aligned}$$

For any time instant t, block matrices F_1 and F_4 are invertible having eigenvalues with pure negative real parts; F_2 and F_3 are non-zero matrices. It can be simplified to an m-dimensional system

$$\frac{d}{dt} \dot{\delta}_m = m_P (F_1 - F_2 F_4^{-1} F_3) \dot{\delta}_m = m_P F_{sim} \dot{\delta}_m.$$

Based on Lemma *4, the simplified matrix F_{sim} preserves this property for any time instant t.*

Since F_{sim} is still a Metzler matrix with zero row sums,

then the proof of asymptotic frequency synchronization is identical for networks either with or without pure load buses. As long as frequencies at buses tied to inverter-based DGs converge, pure load buses would average frequencies of neighboring buses to the same value as well.

For the simplicity of notation, the dynamics is written as $\frac{d}{dt}\dot{\delta}_m = m_P F(t)\dot{\delta}_m$. *Taking the* m*th bus as a reference, then it is possible to rewrite the* m*-dimensional system into a* $(m-1)$*-dimensional one as follows*

$$\frac{d}{dt}\begin{pmatrix} \dot{\delta}_1 - \dot{\delta}_m \\ \dot{\delta}_2 - \dot{\delta}_m \\ \vdots \\ \dot{\delta}_{m-1} - \dot{\delta}_m \end{pmatrix} = m_P F_{m-1}(t) \begin{pmatrix} \dot{\delta}_1 - \dot{\delta}_m \\ \dot{\delta}_2 - \dot{\delta}_m \\ \vdots \\ \dot{\delta}_{m-1} - \dot{\delta}_m \end{pmatrix}.$$

where each element $F_{m-1,ij} = F_{ij} - F_{mj}$. *Subtracting non-negative off-diagonal components of the* m*th row* F_{mj} *for* $j \in \{1, 2, \ldots, m-1\}$ *shift components on the other* $(m-1)$ *rows to the negative direction. Based on Gershgorin theorem, matrix* $F_{m-1}(t)$ *has all its eigenvalues with negative real parts for every time instant* t. *The time-varying dynamic system above can be rewritten as*

$$\frac{d}{dt}\begin{pmatrix} \dot{\theta}_1 \\ \dot{\theta}_2 \\ \vdots \\ \dot{\theta}_{m-1} \end{pmatrix} = m_P F_{m-1}(t) \begin{pmatrix} \dot{\theta}_1 \\ \dot{\theta}_2 \\ \vdots \\ \dot{\theta}_{m-1} \end{pmatrix}.$$

Define a candidate Lyapunov function $V_{\dot{\theta}} = \dot{\theta}_{m-1}^T \dot{\theta}_{m-1}$, *then it is bounded as* $k_1\|\dot{\theta}_{m-1}\|_2^2 \le V_{\dot{\theta}} \le k_2\|\dot{\theta}_{m-1}\|_2^2$, *where* k_1 *and* k_2 *are positive constants. There is* $\dot{V}_{\dot{\theta}} = \dot{\theta}_{m-1}^T[(\dot{F}_{m-1}^T(t) + \dot{F}_{m-1}(t)) + m_P(F_{m-1}^T(t) + F_{m-1}(t))]\dot{\theta}_{m-1}$. *Although symmetric matrix* $(\dot{F}_{(n-1)}^T + \dot{F}_{(n-1)})$ *is not definite, negative definite matrix* $m_P(F_{m-1}^T(t) + F_{m-1}(t))$ *dominates the weighting function, so that* $\dot{V}_{\dot{\theta}}$ *is bounded by* $\dot{V}_{\dot{\theta}} \le -k_3\|\dot{\theta}_{m-1}\|_2^2$ *with* $k_3 > 0$. *Since* k_1, k_2, *and* k_3 *are all positive constants, according to theorem 4.10 in [11], there is* $\dot{\theta}_i$ *asymptotically converging to zero, i.e. each* $\theta_i(t) = \delta_i(t) - \delta_m(t)$ *converges to a constant value.*

Based on the hybrid network model of phase angles, by applying $(\dot{\delta}_i - \dot{\delta}_m)$ *for each* $i \in \{1, 2, \ldots, m-1\}$, *there is*

$$\dot{\delta}_i - \dot{\delta}_m = (\omega_i - \omega_m) - m_P\Big(\sum_{\substack{j=1 \\ j\neq i}}^{m} E_i E_j |Y_{ij}| \sin(\delta_i - \delta_j + \phi_{ij}) - \sum_{j=1}^{m-1} E_m E_j |Y_{mj}| \sin(\delta_m - \delta_j + \phi_{mj})\Big).$$

A linearized model for phase angle analysis can be derived with respect to the equilibrium point θ_{equ}. *There is an* $(m-1)$*-dimensional model as follows*

$$\begin{pmatrix} \dot{\tilde{\theta}}_1 \\ \dot{\tilde{\theta}}_2 \\ \vdots \\ \dot{\tilde{\theta}}_{m-1} \end{pmatrix} = m_P F_{m-1}(t) \begin{pmatrix} \tilde{\theta}_1 \\ \tilde{\theta}_2 \\ \vdots \\ \tilde{\theta}_{m-1} \end{pmatrix}.$$

where each element $F_{m-1,ij} = F_{ij} - F_{mj}$. *For the linearized phase angle difference model above, a Lyapunov function can be defined as* $V_{\tilde{\theta}} = \tilde{\theta}_{m-1}^T \tilde{\theta}_{m-1}$, *bounded as* $k_1^{'}\|\tilde{\theta}_{m-1}\|_2^2 \le V_{\tilde{\theta}} \le k_2^{'}\|\tilde{\theta}_{m-1}\|_2^2$, *where* $k_1^{'}$ *and* $k_2^{'}$ *are positive constants. The time derivative of this Lyapunov function is* $\dot{V}_{\tilde{\theta}} = \tilde{\theta}_{m-1}^T[(\dot{F}_{m-1}^T(t) + \dot{F}_{m-1}(t)) + m_P(F_{m-1}^T(t) + F_{m-1}(t))]\tilde{\theta}_{m-1}$. *Negative definite matrix* $m_P(F_{m-1}^T(t) + F_{m-1}(t))$ *dominates indefinite* $(\dot{F}_{m-1}^T(t) + \dot{F}_{m-1}(t))$, *leading to a bounded* $\dot{V}_{\tilde{\theta}} \le -k_3^{'}\|\tilde{\theta}_{m-1}\|_2^2$ *with* $k_3^{'} > 0$. *Since* $k_1^{'}$, $k_2^{'}$, *and* $k_3^{'}$ *are all positive constants, according to theorem 4.10 in [11], there is asymptotic convergence of phase angle differences* $\tilde{\theta}_{m-1}(t)$ *to a zero vector. Since the linear model is with respect to* θ_{equ}, *then phase angle differences* $\theta_{m-1}(t)$ *converge asymptotically to the equilibrium point to* θ_{equ}. *Based on asymptotic stability theorem in [11], the original nonlinear system model is asymptotically stable with respect to* θ_{equ}.

Remark 4 *Equation (24) bounds the ratio* $|G_{ij}/B_{ij}|$ *of the weakest link within the network. Satisfying this condition ensures phase angle differences* $\theta(t)$ *converging to* θ_{equ}, *once phase shifts reduce within the bound of* $(\frac{\pi}{2} - \alpha_{max})$.

As long as the phase angle differences asymptotically converge to an equilibrium point θ_{equ}, voltage magnitudes of each bus are also asymptotically stabilized. The proof of *Theorem* 7 is decoupled from asymptotic voltage stability analysis. The following theorem establishes the asymptotic voltage stability.

Theorem 9 *Assume that conditions in* Lemma *2 and 3 as well as* Theorem *7 hold, then there is phase angle differences* θ *converging to* θ_{equ} *and voltage magnitudes within invariant set* $\mathcal{I}_E$. *Define* B_1 *and* B_2 *as*

$$B_1 = \frac{K_Q}{m_Q} + \min_i(Q_{load,b,i} + (E_{equ,i} + E_i)Q_{load,a,i}),$$
$$B_2 = m_E.$$

If there is $B_1 > B_2$, (25)

then vector $\{E_i\}$ *asymptotically converges to* $\{E_{equ,i}\}$.

Proof 10 *Because there is an algebraic relationship between $\tilde{Q}_i$ and $\tilde{E}_i$ for pure load buses, as shown in equation (15), it is only necessary to consider only buses with voltage droop control mechanisms. Define a positive function $V_E = \sum_{i=1}^{m} \frac{1}{2m_Q}\tilde{E}_i^2$. Taking the derivative of V_E, there is*

$$\begin{aligned}\dot{V}_E &= \sum_{i=1}^{m} \frac{1}{m_Q}\tilde{E}_i\dot{\tilde{E}}_i, \\ &= \tilde{Q}^T\tilde{E} \\ &\quad -\tilde{E}^T \mathrm{diag}(\frac{\mathrm{K_Q}}{\mathrm{m_Q}} + \mathrm{Q_{load,b,i}} + (\mathrm{E_{equ,i}} + \mathrm{E_i})\mathrm{Q_{load,a,i}})\tilde{\mathrm{E}}.\end{aligned}$$

Because Lemma *3 and* Theorem *7 imply convergence of vector $\{\theta_i\}$ to $\{\theta_{equ,i}\}$, for any ϵ_θ there is a time T such that when $t > T$ there is $|\tilde{\theta}_i|_{max} = |\theta_i - \theta_{equ,i}|_{max} < \epsilon_\theta$. Due to* Lemma *6, $\|\tilde{Q}\|_2$ is bounded above by $m_E\|\tilde{E}\|_2 + \sqrt{m}m_\theta\epsilon_\theta$. As a result, the derivative of V_E is bounded as,*

$$\begin{aligned}\dot{V}_E &\le \sqrt{m}m_\theta\epsilon_\theta \sum_{i=1}^{m} |\tilde{E}_i| \\ &\quad + \tilde{E}^T \mathrm{diag}(\mathrm{m_E} - \frac{\mathrm{K_Q}}{\mathrm{m_Q}} - \mathrm{Q_{load,b,i}} - (\mathrm{E_{equ,i}} + \mathrm{E_i})\mathrm{Q_{load,a,i}})\tilde{\mathrm{E}}.\end{aligned}$$

For an arbitrary ϵ_θ, there is a subset of $\tilde{E}(t)$ satisfying

$$|\tilde{E}_i| < \frac{2\sqrt{m}m_\theta\epsilon_\theta}{-m_E + \frac{K_Q}{m_Q} + Q_{load,b,i} + (E_{equ,i} + E_i)Q_{load,a,i}},$$

for all $i \in \{1, 2, \ldots, m\}$. Under the theorem's assumption in equation (25), the denominator in the equation above is positive. Once $\tilde{E}(t)$ enters the subset at $t = T$, it stays in the set thereafter, i.e. the system is uniformly ultimately bounded. As ϵ_θ goes to zero, T increases and the size of the ultimate bound asymptotically goes to a zero vector. This is sufficient to imply asymptotic convergence of $\tilde{E}$ to zero, which further implies voltage stability. As a result, the voltage control block ensures the asymptotic convergence of voltage magnitudes $\{E_i\}$ to $\{E_{equ,i}\}$.

Remark 5 *Equation (25) bounds control authorities of voltage controllers K_Q/m_Q. As long as voltage control authority is sufficient, voltage magnitudes asymptotically converge to the unique equilibrium point E_{equ}.*

Theorem 11 *Assume that conditions in* Lemma *2 and 3, as well as* Theorem *7 and 9 hold, then $\lim_{t\to\infty}\dot{\delta}_1(t) = \ldots = \lim_{t\to\infty}\dot{\delta}_n(t) = \omega_{equ}$ so that there is asymptotic frequency synchronization.*

Proof 12 *Since conditions in* Lemma *2 and 3, as well as* Theorem *7 and 9 are all satisfied, then there is phase angle differences θ converging to θ_{equ} and voltage magnitudes E converging to E_{equ}. Based on power balance relationships in equations (2,3), real and reactive power P and Q also converge to P_{equ} and Q_{equ}, respectively. Since $P \to P_{equ}$ and $E \to E_{equ}$, phase angle dynamics in equation (6) is written as,*

$$\lim_{t\to\infty}\dot{\delta}_i(t) = m_P(P_{ref,i} - P_{equ,i} - P_{load,i}(E_{equ,i})) + \omega_0.$$

Bring expression of $P_{ref,i}$ in equation (12), for each bus i there is

$$\lim_{t\to\infty}\dot{\delta}_i(t) = m_P(\frac{1}{m_P}(\omega_{equ} - \omega_0)) + \omega_0 = \omega_{equ}.$$

Frequency at each DG-coupled bus converges to the equilibrium ω_{equ}. Since frequencies on pure load buses are averages of their neighboring buses, the all n buses have $\lim_{t\to\infty}\dot{\delta}_1(t) = \ldots = \lim_{t\to\infty}\dot{\delta}_n(t) = \omega_{equ}$, i.e. converging to the same ω_{equ}.

4.3 Extension to Grid-Connected Scenarios

To extend our analysis from islanded networks to general grid cases, a grid connection point must be included, which can be treated as an infinite bus. Different from a droop-controlled DG, this infinite bus maintains voltage and compensates for any real power imbalance. Such an infinite bus is approximated as a bus tied to inverter based DGs, whose control strengths of both phase angle and voltage, represented as m_p and K_Q/m_Q, are infinite. Stability conditions are then naturally satisfied, with other buses controlled by droop controllers. Therefore, our stability analysis extends to grid-connected cases.

5 Simulation Experiments

Simulation tests are conducted in a modified IEEE standard 37-bus distribution network. Two simulation models with different SCR values are introduced. One model has an SCR of around 1000, i.e. a *strong* network; the other model is a stressed *weak* network with its SCR being around six. Simulation results show that the stability conditions derived in this paper ensure stability for stressed weak networks, even after recovering from disturbances such as load changes and voltage impulses. Without conditions on voltage control, although *strong* networks can recover from impulse disturbances on DG's voltage magnitudes, stressed *weak* networks cannot stabilize anymore. Therefore, stability conditions derived for strong networks, without considering voltage control, is not sufficient to assure asymptotic stability of weak networks.

Based on the standard test feeder in [10], demonstrated in Figure 4, the 4.8kV strong network has three modifications: a) the unbalanced network is modified such that all pure load buses except bus 1 are with 100kW of three-phase balanced constant impedance load; b) there

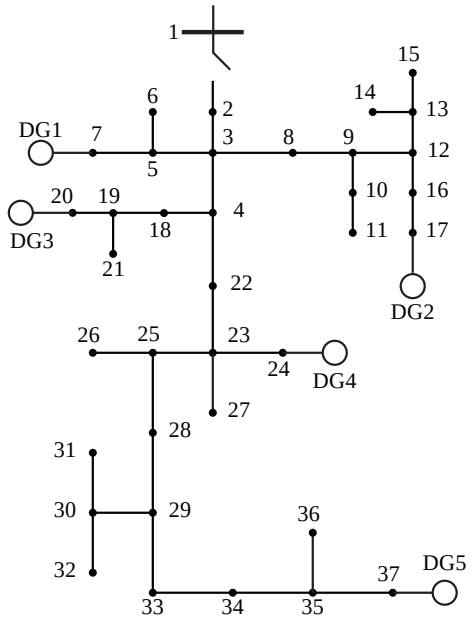

Fig. 4. Simulation 37-bus Test Feeder with 5 Distributed Generations

are five additional DGs coupled at the ends of distribution feeders, with a total capacity sufficient to supply all loads; c) cables used to connect inverter-based DGs are 200 feet "724" cables, as defined in [19]. Compared with the strong network model, the weak network operates at 480V and has its connections cables to DGs extended to 1000 feet.

In the first place, satisfying the sufficient stability conditions ensures that the DG-coupled distribution network asymptotically converges to an equilibrium point. In the strong network, equilibrium points conform to regulatory limits of frequency around 60Hz and voltage within $[0.95, 1.05]$ p.u.. An optimal power flow (OPF) problem is formed to calculate the equilibrium point. The solution has its frequency $\omega_{equ} = 60$Hz, all voltage magnitudes stay between 0.997p.u. and 1.003p.u.. Conditions in *Lemma* 2 requires that $K_Q \geq 111388$, with $m_Q = 0.05$. The Jacobian in *Lemma* 1 is full rank, and conditions in *Lemma* 3, *Theorem* 7, and *Theorem* 9 are all satisfied.

The following simulation test starts from connecting to the main grid; at $t = 50s$, the test feeder is islanded from the main grid by opening the primary switch between bus 1 and 2; at $t = 75s$, the load on all pure load buses increase by 50% for five seconds. Both network frequency and voltage magnitudes converge to the equilibrium point, as shown in figure 5.

In the left plot in figure 5, the upper and lower dash lines are the maximum and minimum voltages among all buses. The solid line represents the voltage magnitude at bus 2. In the right plot, network frequency is demonstrated in blue line, with a 60Hz nominal value. During the islanding operation at $t = 50s$, the voltage envelop does not change. Within five seconds after islanding, both voltage magnitudes and network frequency converge to the equilibrium point. After the load increase at $t = 75s$, the maximum voltage decrease is less than 0.003p.u., and the network frequency droops by as much as 3.31×10^{-6}Hz. In less than five seconds after all loads return to nominal values, network states restore to the equilibrium point.

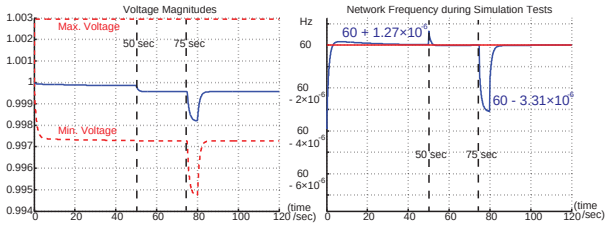

Fig. 5. Simulation Result of DG-coupled 37-bus Test Feeder Response to Changing Loads

The following simulations show network response to voltage magnitude changes on buses tied to DGs in figure 6. After the test feeder islands from the main grid at $t = 50s$, network states converge to the equilibrium point in five seconds. At $t = 75s$, the voltage magnitude at DG 1 is decreased by 0.9p.u. and increased by 1.1p.u.. The network response is shown as in figure 6

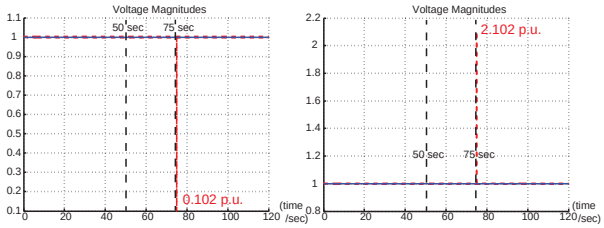

Fig. 6. Simulation Result of DG-coupled 37-bus Test Feeder Response to Voltage Changes at DGs

In the left plot of figure 6, the minimum voltage envelop drops to 0.102p.u., in response to a 0.9p.u. voltage drop at DG 1. Voltage magnitudes restore to the equilibrium point in less than two seconds, so as the network frequency. In the right plot, the maximum voltage increases to 2.102p.u., after the voltage magnitude at DG 1 increases by 1.1p.u.. Restoration of voltage and frequency takes less than two seconds.

Both simulation tests demonstrate that satisfying stability conditions derived earlier, system states of a DG-coupled power distribution network asymptotically converge to the equilibrium point designated. Even after load changes on pure load buses and voltage magnitude changes on DGs, system states restore to $(P_{equ}, Q_{equ}, \theta_{equ}, E_{equ}, \omega_{equ})$.

For the strong network, if voltage control condition is relaxed such that K_Q is only 1% of the original value, system states are still able to restore to the designated equilibrium point. Voltage impulse disturbances are again applied to this network, such that the voltage magnitude at DG 1 is decreased by 0.9p.u. and increased by 1.1p.u.. The network response is shown as in figure 7

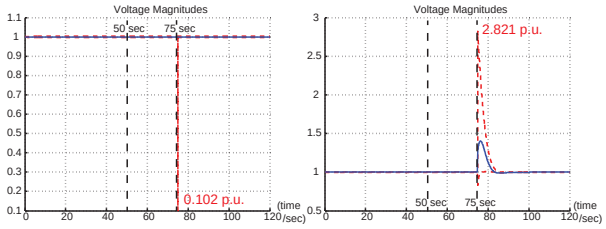

Fig. 7. Simulation Result of DG-coupled 37-bus Test Feeder Response to Voltage Changes at DGs with Decreased K_Q

In the left plot of figure 7, the minimum voltage envelop drops to 0.102p.u., in response to a 0.9p.u. voltage drop at DG 1. Voltage magnitudes restore to the equilibrium point in less than two seconds, so as the network frequency. In the right plot, the maximum voltage increases to 2.821p.u., after the voltage magnitude at DG 1 increases by 1.1p.u.. Restoration of voltage and frequency takes less than ten seconds. It is demonstrated that strong networks can recover from voltage disturbances, even if stability conditions for voltage control are relaxed.

In the weak network, whose SCR is as small as six, satisfying the sufficient stability conditions ensures that the DG-coupled distribution network asymptotically converges to an equilibrium point. The equilibrium point is still at 60Hz, while voltage regulatory limits of $\pm 5\%$ are relaxed. An OPF problem is formed to calculate the equilibrium point, whose voltage magnitudes stay between 0.73p.u. and 1.33p.u.. Conditions in *Lemma* 2 requires that $K_Q \geq 1476$, with $m_Q = 0.05$. The Jacobian in *Lemma* 1 is full rank, and conditions in *Lemma* 3, *Theorem* 7, and *Theorem* 9 are all satisfied. Both load level and voltage magnitude disturbances are applied to the weak network, using the same procedure as in the strong network.

In response to load level changes, both network frequency and voltage magnitudes converge to the equilibrium point, as shown in figure 8.

In the left plot in figure 8, the upper and lower red dash lines are the maximum and minimum voltages among all buses. The blue line represents the voltage magnitude at bus 2. In the right plot, network frequency is demonstrated in blue line, with a 60Hz nominal value. During the islanding operation at $t = 50s$, the voltage envelop does not change. Within five seconds after islanding, both voltage magnitudes and network frequency converge to the equilibrium point. After the load increase at $t = 75s$, the maximum voltage decrease is less than

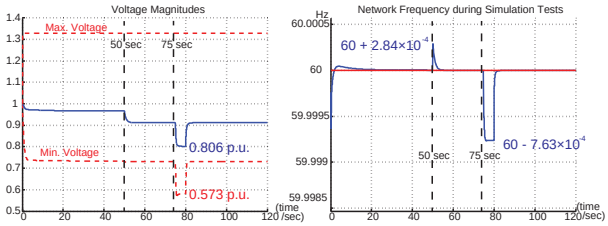

Fig. 8. Simulation Result of Weak Network Response to Changing Loads

0.15p.u., and the network frequency droops by as much as 7.63×10^{-4}Hz. In less than five seconds after all loads return to nominal values, network states restore to the equilibrium point.

In response to voltage magnitude changes at DG 1, the weak network response is shown as in figure 9

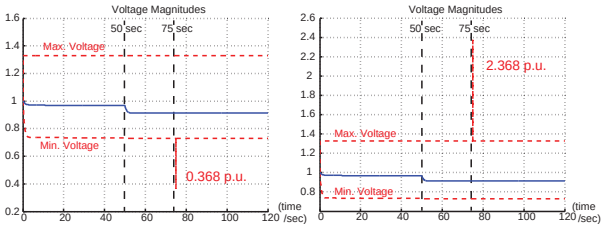

Fig. 9. Simulation Result of Weak Network Response to Voltage Changes at DGs

In the left plot of figure 9, the minimum voltage envelop drops to 0.368p.u., in response to a 0.9p.u. voltage drop at DG 1. Voltage magnitudes restore to the equilibrium point in less than two seconds, so as the network frequency. In the right plot, the maximum voltage increases to 2.368p.u., after the voltage magnitude at DG 1 increases by 1.1p.u.. Restoration of voltage and frequency takes less than two seconds.

It is demonstrated that, asymptotic stability and frequency synchronization are ensured in stressed weak networks, after load changes and voltage impulses on DG-coupled buses. By reducing voltage control K_Q from 1476 to 200, the weak network is not able to recover from voltage magnitude disturbances. Stability conditions in weak networks are not as conservative as in strong ones. This phenomenon matches our stability analysis, where strong network assumptions are relaxed for weak networks with small SCR values. Stability conditions derived for strong networks, without considering voltage control, is not sufficient to assure asymptotic stability of weak networks.

6 Summary and Future Work

Asymptotic stability conditions are derived for DG-coupled power distribution networks, when the network interconnections are *weak*. These conditions take

the form of inequality constraints on various network parameters, loads and generation control commands. These conditions can therefore be easily incorporated into optimal dispatch problems.

These stability conditions have the advantage of ensuring stability under stochastic load and generation situations for weak networks. By incorporating these stability conditions with OPF problems, intermittent renewable DGs can be efficiently managed. Asymptotic voltage stability and frequency synchronization are ensured, without the computational burden of applying model predictive control algorithms. Relevant work will be demonstrated in another paper.

References

[1] Podmore R Athay, T and S Virmani. A practical method for the direct analysis of transient stability. *Power Apparatus and Systems, IEEE Transactions on*, (2):573–584, 1979.

[2] Arthur R BERGEN and Vijay VITTAL. *Power systems analysis*. 1999.

[3] F. Dörfler and F. Bullo. On the critical coupling for kuramoto oscillators. *SIAM Journal on Applied Dynamical Systems*, 10(3):1070–1099, 2011.

[4] F. Dorfler and F. Bullo. Synchronization and transient stability in power networks and non-uniform Kuramoto oscillators. 50(3):1616–1642, 2012.

[5] AH El-Abiad and K Nagappan. Transient stability regions of multimachine power systems. *Power Apparatus and Systems, IEEE Transactions on*, (2):169–179, 1966.

[6] Klaus Fritzsche and Hans Grauert. *From holomorphic functions to complex manifolds*, volume 213. Springer, 2002.

[7] GE Gless. Direct method of liapunov applied to transient power system stability. *Power Apparatus and Systems, IEEE Transactions on*, (2):159–168, 1966.

[8] M. Illindala and G. Venkataramanan. Small signal stability of a microgrid with parallel connected distributed generation. *Intellegent Automation and Soft Computing*, 16(2):231–250, 2010.

[9] Florian Dorfler John W. Simpson-Porco and Francesco Bullo. Synchronization and power sharing for droop-controlled inverters in islanded microgrids. *Automatica*, 49(9):2603 – 2611, 2013.

[10] William H Kersting. Radial distribution test feeders. In *Power Engineering Society Winter Meeting, 2001. IEEE*, volume 2, pages 908–912. IEEE, 2001.

[11] Hassan K Khalil. *Nonlinear systems*, volume 3. Prentice hall Upper Saddle River, 2002.

[12] Rogers-GJ Wong DY Wang L Kundur, P and MG Lauby. A comprehensive computer program package for small signal stability analysis of power systems. *Power Systems, IEEE Transactions on*, 5(4):1076–1083, 1990.

[13] R.H. Lasseter. Smart distribution: Coupled microgrids. *Proceedings of the IEEE*, 99(6):1074–1082, 2011.

[14] Nelson Martins. Efficient eigenvalue and frequency response methods applied to power system small-signal stability studies. *Power Systems, IEEE Transactions on*, 1(1):217–224, 1986.

[15] IEEE Task Force on Load Representation for Dynamic Performance. Load representation for dynamic performance analysis [of power systems]. *Power Systems, IEEE Transactions on*, 8(2):472–482, 1993.

[16] RJ Plemmons. M-matrix characterizations. inonsingular m-matrices. *Linear Algebra and its Applications*, 18(2):175–188, 1977.

[17] Anta Adolfo Trung Truong Duc Raisch Jorg Schiffer, Johannes and Tevfik Sezi. On power sharing and stability in autonomous inverter-based microgrids. In *Decision and Control (CDC), 2012 IEEE 51st Annual Conference on*, pages 1105–1110. IEEE, 2012.

[18] Nicholas PW Strachan and Dragan Jovcic. Stability of a variable-speed permanent magnet wind generator with weak ac grids. *Power Delivery, IEEE Transactions on*, 25(4):2779–2788, 2010.

[19] Distribution System Analysis Subcommittee. Ieee 37 node test feeder. Technical report, IEEE, 2001.

[20] Li X Sun, YZ and YH Song. A new lyapunov function for transient stability analysis of controlled power systems. In *Power Engineering Society Winter Meeting, 2000. IEEE*, volume 2, pages 1325–1330. IEEE, 2000.

[21] Liu QJ Song YH Sun, YZ and TL Shen. Hamiltonian modelling and nonlinear disturbance attenuation control of tcsc for improving power system stability. *IEE Proceedings-Control Theory and Applications*, 149(4):278–284, 2002.

[22] Paulo Tabuada and George J Pappas. From nonlinear to hamiltonian via feedback. In *Decision and Control, 2002, Proceedings of the 41st IEEE Conference on*, volume 2, pages 1515–1520. IEEE, 2002.

[23] Kemp Murray C Uekawa, Yasuo and Leon L Wegge. P- and pn-matrices, minkowski- and metzler- matrices, and generalizations of the stolper-samuelson and samuelson-rybczynski theorems. *Journal of International Economics*, 3(1):53–76, 1973.

[24] Lei Wang and Adam Semlyen. Application of sparse eigenvalue techniques to the small signal stability analysis of large power systems. In *Power Industry Computer Application Conference, 1989. PICA'89, Conference Papers*, pages 358–365. IEEE, 1989.

[25] Xia Meng Wang, Zhao and Michael Lemmon. Voltage stability of weak power distribution networks with inverter connected sources. In *American Control Conference, Washington DC, USA*, 2013.

[26] JL Willems and JC Willems. The application of lyapunov methods to the computation of transient stability regions for multimachine power systems. *Power Apparatus and Systems, IEEE Transactions on*, (5):795–801, 1970.

A Lemmas

In the Appendix, *Lemma* 5 and *Lemma* 6 establish bounds on norms of $\tilde{Q}$ as functions of voltage and phase angle error vectors, i.e. $\tilde{E}$ and $\tilde{\theta}$.

Lemma 5 *Defined* l_E *and* l_θ *as*

$$l_E = 2(\max_i(E_{equ,i}) + |\tilde{E}_i|_{max})(|G_{ii}|_{max} + 2|B_{ii}|_{max}),$$
$$l_\theta = 2(\max_i(E_{equ,i}) + |\tilde{E}_i|_{max})^2(|G_{ii}|_{max} + |B_{ii}|_{max}),$$

then absolute value of the reactive power error $|\tilde{Q}_i|$ is bounded by

$$|\tilde{Q}_i| \leq l_E |\tilde{E}_i|_{max} + l_\theta \cdot 2\pi. \tag{A.1}$$

Proof 13 *With the help of its Jacobian $\partial Q/\partial E$ and $\partial Q/\partial\theta$, $\tilde{Q}$ is linearized as $\tilde{Q} = Q - Q_{equ} = \frac{\partial Q}{\partial E}\Big|_{equ}(E - E_{equ}) + \frac{\partial Q}{\partial \theta}\Big|_{equ}(\theta - \theta_{equ}) = \frac{\partial Q}{\partial E}\Big|_{equ}\tilde{E} + \frac{\partial Q}{\partial \theta}\Big|_{equ}\tilde{\theta}$. Taking infinite vector norms on both sides, there is*

$$\begin{aligned}
\|\tilde{Q}\|_\infty &\leq \left\|\frac{\partial Q}{\partial E}\tilde{E} + \frac{\partial Q}{\partial \theta}\tilde{\theta}\right\|_\infty \leq \left\|\frac{\partial Q}{\partial E}\tilde{E}\right\|_\infty + \left\|\frac{\partial Q}{\partial \theta}\tilde{\theta}\right\|_\infty, \\
&\leq \left\|\frac{\partial Q}{\partial E}\right\|_\infty \left\|\tilde{E}\right\|_\infty + \left\|\frac{\partial Q}{\partial \theta}\right\|_\infty \left\|\tilde{\theta}\right\|_\infty, \\
\max_i(|\tilde{Q}_i|) &\leq \left\|\frac{\partial Q}{\partial E}\right\|_\infty \max_i(|\tilde{E}_i|) + \left\|\frac{\partial Q}{\partial \theta}\right\|_\infty \max_i(|\tilde{\theta}_i|),
\end{aligned}$$

where $\|\frac{\partial Q}{\partial E}\|_\infty$ and $\|\frac{\partial Q}{\partial \theta}\|_\infty$ are bounded as following

$$\begin{aligned}
&\|\frac{\partial Q}{\partial E}\|_\infty \\
&= \sum_{\substack{j=1 \\ j\neq i}} |E_i(G_{ij}\sin(\theta_i - \theta_j) - B_{ij}\cos(\theta_i - \theta_j))| \\
&+ |\sum_{\substack{j=1 \\ j\neq i}} E_i(G_{ij}\sin(\theta_i - \theta_j) - B_{ij}\cos(\theta_i - \theta_j)) - 2E_iB_{ii}|, \\
&\leq |2E_iB_{ii}| + 2\sum_{\substack{j=1 \\ j\neq i}} |E_i(G_{ij}\sin(\theta_i - \theta_j) - B_{ij}\cos(\theta_i - \theta_j))|, \\
&\leq 2\max_i(|E_i|)[|B_{ii}|_{max} + \max_i(\sum_{\substack{j=1 \\ j\neq i}}(|G_{ij}| + |B_{ij}|))], \\
&\leq 2(\max_i(E_{equ,i}) + \max_i(|\tilde{E}_i|))(|G_{ii}|_{max} + 2|B_{ii}|_{max}) = l_E,
\end{aligned}$$

$$\begin{aligned}
&\|\frac{\partial Q}{\partial \theta}\|_\infty \\
&= |\sum_{\substack{j=1 \\ j\neq i}} E_iE_j(G_{ij}\cos(\theta_i - \theta_j) + B_{ij}\sin(\theta_i - \theta_j))| \\
&+ \sum_{\substack{j=1 \\ j\neq i}} |E_iE_j(G_{ij}\cos(\theta_i - \theta_j) + B_{ij}\sin(\theta_i - \theta_j))|, \\
&\leq 2\sum_{\substack{j=1 \\ j\neq i}} |E_iE_j(G_{ij}\cos(\theta_i - \theta_j) + B_{ij}\sin(\theta_i - \theta_j))|, \\
&\leq 2(\max_i(|E_i|))^2 \max_i(\sum_{\substack{j=1 \\ j\neq i}}(|G_{ij}| + |B_{ij}|)), \\
&\leq 2(\max_i(E_{equ,i}) + \max_i(|\tilde{E}_i|))^2(|G_{ii}|_{max} + |B_{ii}|_{max}) = l_\theta.
\end{aligned}$$

Remark 6 *Absolute value of reactive power error $|\tilde{Q}_i|$ is bounded as a function of equilibrium voltage magnitude $E_{equ,i}$, network link parameters G_{ii} and B_{ii}, as well as maximum voltage error $|\tilde{E}_i|$.*

Lemma 6 *Define m_E and m_θ as*

$$\begin{aligned}
m_E &= \max\{\sqrt{\lambda} : \lambda \text{ is an eigenvalue of } (\partial Q/\partial E)^*(\partial Q/\partial E)\}, \\
m_\theta &= \max\{\sqrt{\lambda} : \lambda \text{ is an eigenvalue of } (\partial Q/\partial \theta)^*(\partial Q/\partial \theta)\},
\end{aligned}$$

then two-norm of the reactive power error vector $\tilde{Q}$ is bounded by

$$\|\tilde{Q}\|_2 \leq m_E\|\tilde{E}\|_2 + \sqrt{n}m_\theta|\tilde{\theta}_i|_{\max}. \tag{A.2}$$

Proof 14 *If system frequency synchronizes to ω_{equ} and phase shifts are within the invariant set $\mathcal{I}_\theta$, then for any $i \in \{1, 2, \ldots, n\}$ there is a bounded $|\tilde{\theta}_i|$. Within the invariant set $\mathcal{I}_E$, applying vector two-norm and its induced matrix two-norm, there is*

$$\begin{aligned}
\|\tilde{Q}\|_2 &= \|\frac{\partial Q}{\partial E}\tilde{E} + \frac{\partial Q}{\partial \theta}\tilde{\theta}\|_2, \\
&\leq \|\frac{\partial Q}{\partial E}\tilde{E}\|_2 + \|\frac{\partial Q}{\partial \theta}\tilde{\theta}\|_2, \\
&\leq \|\frac{\partial Q}{\partial E}\|_2\|\tilde{E}\|_2 + \|\frac{\partial Q}{\partial \theta}\|_2\sqrt{n}\max_i(|\tilde{\theta}_i|), \\
&\leq m_E\|\tilde{E}\|_2 + \sqrt{n}m_\theta \max_i(|\tilde{\theta}_i|).
\end{aligned}$$

Remark 7 *Magnitude of reactive power error vector $\|\tilde{Q}\|_2$ is bounded as a weighted combination of voltage magnitude error vector magnitude $\|\tilde{E}\|_2$ and the maximum phase angle error $|\tilde{\theta}_i|$.*

As a result of *Lemma* 5 and *Lemma* 6, it is possible to bound ∞-norm and 2-norm of error states of reactive power $\tilde{Q}$. These bounds take forms of inequalities of voltage error and phase angle error magnitudes, which are used later in deriving stability conditions.